Human Molecular Genetics, 2013, Vol. 22, No. 19 **3894–3905**
doi:10.1093/hmg/ddt244
Advance Access published on June 4, 2013

RD3 gene delivery restores guanylate cyclase localization and rescues photoreceptors in the *Rd3* mouse model of Leber congenital amaurosis 12

Laurie L. Molday[1], Hidayat Djajadi[1], Paul Yan[2], Lukasz Szczygiel[3], Sanford L. Boye[4], Vince A. Chiodo[4], Kevin Gregory-Evans[2], Marinko V. Sarunic[3], William W. Hauswirth[4] and Robert S. Molday[1,2,*]

[1]Department of Biochemistry & Molecular Biology, University of British Columbia, Vancouver, BC, Canada V6T1Z3, [2]Department of Ophthalmology and Visual Sciences, University of British Columbia, Vancouver, BC, Canada V5Z 3N9, [3]Department of Molecular Biology & Biochemistry and Engineering Science, Simon Fraser University, Burnaby, BC, Canada V5A 1S6 and [4]Department of Ophthalmology, University of Florida, Gainesville, FL, Canada 32610-0284

Received February 12, 2013; Revised May 15, 2013; Accepted May 26, 2013

RD3 is a 23 kDa protein implicated in the stable expression of guanylate cyclase in photoreceptor cells. Truncation mutations are responsible for photoreceptor degeneration and severe early-onset vision loss in Leber congenital amaurosis 12 (LCA12) patients, the *rd3* mouse and the *rcd2* collie. To further investigate the role of RD3 in photoreceptors and explore gene therapy as a potential treatment for LCA12, we delivered adeno-associated viral vector (AAV8) with a Y733F capsid mutation and containing the mouse *Rd3* complementary DNA (cDNA) under the control of the human rhodopsin kinase promoter to photoreceptors of 14-day-old Rb(11.13)4Bnr/J and In (5)30Rk/J strains of *rd3* mice by subretinal injections. Strong RD3 transgene expression led to the translocation of guanylate cyclase from the endoplasmic reticulum (ER) to rod and cone outer segments (OSs) as visualized by immunofluorescence microscopy. Guanylate cyclase expression and localization coincided with the survival of rod and cone photoreceptors for at least 7 months. Rod and cone visual function was restored in the In (5)30Rk/J strain of *rd3* mice as measured by electroretinography (ERG), but only rod function was recovered in the Rb(11.13)4Bnr/J strain, suggesting that the latter may have another defect in cone phototransduction. These studies indicate that RD3 plays an essential role in the exit of guanylate cyclase from the ER and its trafficking to photoreceptor OSs and provide a 'proof of concept' for AAV-mediated gene therapy as a potential therapeutic treatment for LCA12.

INTRODUCTION

Leber congenital amaurosis (LCA) is a genetically and clinically heterogeneous group of severe early-onset disorders that constitute ~5% of inherited retinal degenerative diseases (1). Infants are typically diagnosed with LCA shortly after birth on the basis of severe loss in visual function, nystagmus, slow pupillary response and a reduced or nondetectable electroretinogram (ERG). To date, mutations in 17 different genes have been linked to autosomal recessive forms of LCA. Proteins encoded by LCA genes function in diverse cellular pathways crucial for photoreceptor cell structure, function and survival including phototransduction, vitamin A metabolism, vesicle trafficking, protein assembly, ciliary structure and transport, photoreceptor development and morphogenesis, guanine nucleotide synthesis and outer segment (OS) phagocytosis.

Mutations in the *GUCY2D* gene encoding guanylate cyclase 1 (GC1, also known as RetGC1) were first shown to cause a severe form of LCA now known as LCA1 (2). GC1 is expressed at relatively high levels in the OSs of rod and cone photoreceptor cells, where it catalyzes the synthesis of cGMP from GTP (3–5). Cyclic GMP, the second messenger of phototransduction, controls the influx of Na^+ and Ca^{2+} into photoreceptor OSs by binding to the cyclic nucleotide-gated channel in the plasma

*To whom correspondence should be addressed at: Department of Biochemistry and Molecular Biology, 2350 Health Sciences Mall, University of British Columbia, Vancouver, Canada BC V6T 1Z3. Tel: +1 6048226173; Fax: +1 6048225227; Email: molday@mail.ubc.ca

membrane and consequently plays a central role in calcium homeostasis as well as phototransduction in rod and cone cells (6, 7). Another guanylate cyclase isoform GC2 is expressed at lower levels in rod OSs (8, 9), but to date mutations in this isoform have not been linked to any retinal degenerative disease.

LCA12 is a severe autosomal recessive disease caused by premature stop mutations in the *RD3* gene (10–12). Similar truncation mutations cause early-onset rod and cone degeneration in the *rd3* mouse and the *rcd2* collie, both of which serve as valuable animal models for LCA12 (10, 13). The *RD3* gene encodes a 23 kDa protein containing a putative coil–coil domain and phosphorylation sites. RD3 is highly expressed in rod and cone photoreceptor cells where it interacts with guanylate cyclases GC1 and GC2 (14). In the *rd3* mouse [strain Rb(11.13)4Bnr/J], GC1 and GC2 are undetectable, suggesting that RD3 plays a crucial role in the stable expression of these key phototransduction proteins (14). *In vitro* studies have also shown that RD3 directly inhibits the catalytic activity of GC (15). The phenotype of the *rd3* mouse is similar to that of the GC1/GC2 (GC-E/GC-F) double knockout mouse (4, 14, 16). These studies suggest that the loss in GC expression and/or function may be responsible for photoreceptor degeneration in LCA12 as well as LCA1.

If RD3 is critical for GC expression and subcellular localization and consequently photoreceptor cell survival, then delivery of the normal *RD3* gene to rods and cones of the *rd3* mouse should restore photoreceptor cell function and viability. The goals of this study were (1) to determine whether the delivery of *Rd3* to photoreceptors of the *rd3* mouse can re-establish GC expression and translocation to the OS, and (2) to evaluate gene therapy as a potential therapeutic treatment for LCA12 using the *rd3* mouse as a model system. Here, we show that adeno-associated viral vector (AAV) mediated gene delivery of murine *Rd3* to photoreceptors of *rd3* mice restores GC expression and trafficking to photoreceptor OSs and rescues rod and cone photoreceptor function and survival. We also provide evidence that RD3 functions as a chaperone protein required for the exit of GC from the endoplasmic reticulum (ER) of photoreceptors as part of its trafficking to photoreceptor OSs.

RESULTS

Restoration of guanylate cyclase expression and localization in the 4Bnr strain of *rd3* mice treated with AAV8(Y733F)-hGRK1-*mRd3*

The murine *Rd3* complementary DNA (cDNA) under the control of the human rhodopsin kinase promoter hGRK1 was packaged into AAV8 containing the Y733F surface capsid protein mutation for gene delivery studies. This AAV vector–promoter combination has been shown to produce rapid and high protein expression in murine rod and cone photoreceptors (17–20). The Rb(11.13)4Bnr/J strain (referred to here as 4Bnr) is one of several strains of *rd3* mice, which has a mutation in the *Rd3* gene resulting in an unstable truncated 106 amino acid protein (10, 21). This strain was used in our initial studies, since it has been most widely studied and reported to undergo photoreceptor degeneration at a well-defined rate after postnatal day 14 (P14) with few photoreceptors remaining after postnatal day 100 (P100) (10, 14, 22).

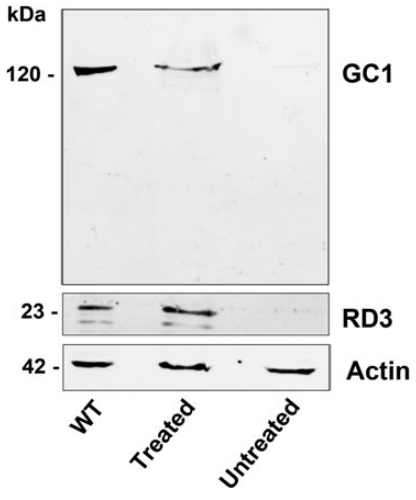

Figure 1. Expression of RD3 and GC1 by western blotting. Retinal extracts from six WT eyes, six AAV8(Y733F)-hGRK1-m*Rd3*-treated eyes and six-untreated 4Bnr-*rd3* eyes were analyzed at 35 days post-injection on SDS gels. Western blots were labeled with the Rd3–9D12 monoclonal antibody for the detection of RD3 and the GC1-8A5 monoclonal antibody for the detection of GC1. Actin labeling was used as a loading control.

AAV8(Y733F)-hGRK1-m*Rd3* was injected into the subretinal space of three 14-day-old 4Bnr *rd3* mice with three untreated *rd3* mice serving as controls. The extent of RD3 expression was monitored on western blots of retinal extracts from the treated and untreated eyes 35 days post-injection and compared with the endogenous level of RD3 in retinal extracts from three age-matched WT mice. The full-length 23 kDa RD3 protein was present in retinal extracts from wild-type (WT) and AAV-treated mice, but absent from untreated 4Bnr *rd3* mice (Fig. 1). The level of RD3 transgene expression was generally comparable with endogenous RD3 expression in WT mouse retinal extracts. The extent of GC1 expression was also measured by probing the western blots with an anti-GC1 monoclonal antibody. A dramatic increase in GC1 expression was observed in the retinal extracts from the AAV-treated eyes with the level of expression reaching 62% that for WT mice.

Previous studies have shown that GC1 and GC2 expression in 4Bnr *rd3* mice is undetectable by immunofluorescence microscopy (14). To determine whether RD3 transgene expression restores endogenous GC1 expression and localization to the photoreceptor OS layer, we labeled retinal cryosections of AAV-treated and -untreated eyes with a GC1-specific antibody for visualization by immunofluorescence microscopy. Strong GC1 expression was observed in six of the AAV8(Y733F)-hGRK1-m*Rd3*-treated mice 2 weeks post-injection with expression extending throughout most of the retina in 60% of the treated eyes (Fig. 2A). In 40% of the cases, GC1 expression was limited to approximately half the retina, most likely due to variability of injection. In contrast, GC1 expression was undetectable in the retina of all untreated mice.

At higher magnification, GC1 correctly localized to the OSs of rod and cone photoreceptor cells of the treated 4Bnr *rd3* eyes, showing a distribution similar to that observed for WT mice (Fig. 2B). A thinning of the outer nuclear layer (ONL) and a reduction in the length of the OS layer were observed for both the

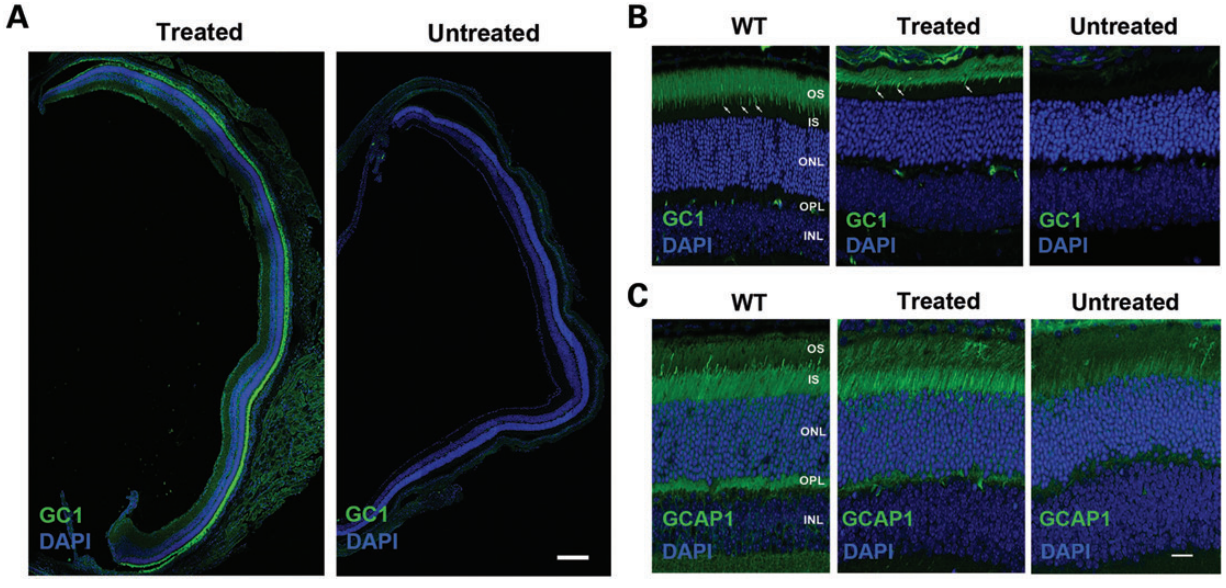

Figure 2. GC1 and GCAP1 expression and localization in the photoreceptors of untreated and treated 4Bnr *rd3* mice by immunofluorescence microscopy. The right eye of a 4Bnr *rd3* mouse was injected (treated) with AAV8(Y733F)-hGRK1-*mRd3* at P14 with the uninjected (untreated) left eye serving as a contralateral control. Retinal cryosections prepared 2 weeks post-injection (P28) were labeled for GC1 or GCAP1 (green) and counterstained with DAPI (blue) nuclear stain. (**A**) Retinal sections from a whole eye at low magnification. GC1 staining is present throughout the retina of the treated, but not the untreated eye. Bar 200 μm. (**B**) GC-labeled retinal sections at higher magnification. GC1 is correctly localized to the rod and cone (arrow) OSs of the treated eye similar to GC1 localization in WT Balb/c mouse retina. (**C**) GCAP1-labeled retinal sections at higher magnification. GCAP1 distribution in the treated retina is similar to that in the WT retina, whereas the untreated retina shows reduced GCAP1 expression primarily in the inner segment. Representative micrographs are shown from analysis of six mice. OS, OS layer; IS, inner segment layer; ONL, outer nuclear layer; OPL, outer plexiform layer; INL, inner nuclear layer. Bar—10 μm.

treated and untreated eyes consistent with some photoreceptor degeneration occurring between P14 and P28.

Guanylate cyclase activating protein, GCAP1, is known to associate with GC1 and regulate its enzymatic activity in a Ca-dependent manner (23, 24). In WT mice, GCAP1 is localized to both the inner and OSs of photoreceptors, whereas in *rd3* mice GCAP1 expression is significantly reduced and primarily found in the inner segments (14, 16) (Fig. 2C). Subretinal injections of AAV8(Y733F)-hGRK1-m*Rd3* resulted in an increase in GCAP1 expression and localization to photoreceptor inner and OSs similar to that observed in WT mice (Fig. 2C).

Long-term expression of GC and rescue of rod photoreceptors in 4Bnr *rd3* mice treated with AAV8(Y733F)-hGRK1-m*Rd3*

Immunofluorescence microscopy and optical coherence tomography (OCT) were used to evaluate long-term GC1 expression and photoreceptor survival in 4Bnr *rd3* mice injected with AAV8(Y733F)-hGRK1-m*Rd3* at P14. Strong GC1 expression and localization to the photoreceptor OS layer persisted through P200 at which time the experiment was terminated (Fig. 3A). This was associated with sustained photoreceptor cell survival as determined by the thickness of the ONL. At P70, the ONL of the untreated retina was reduced to only one to two layers of nuclei and at P200 no photoreceptor nuclei were found, in general agreement with previously reported studies (22). In contrast, the AAV-treated retina had a substantial ONL at both P70 and P200, indicating significant sustained photoreceptor survival. The change in ONL as a function of age is shown for the treated and untreated retinas of *rd3* 4Bnr mice in Figure 3B.

OCT is a noninvasive imaging technique, which can be used to assess the retinal integrity. Representative OCT images of WT, treated and untreated mice are shown in Figure 3C. In agreement with the immunocytochemical studies, preservation of the ONL was observed in AAV8(Y733F)-hGRK1-m*Rd3* treated mice.

In addition to restoring GC1 expression, subretinal delivery of murine *Rd3* also restored long-term expression and localization of GC2 in OSs of rod photoreceptors (Fig. 4A). The effect of *Rd3* transgene delivery on the distribution of other photoreceptor OS proteins was also investigated by immunofluorescence microscopy. The rod cyclic nucleotide-gated channel (CNGA1), peripherin/rds and phosphodiesterase 6 (PDE6) correctly localized to the photoreceptor OS layer with the CNGA1 and PDE6 expressed in rod photoreceptors and peripherin/rds present in both rod and cone photoreceptor cells (Fig. 4B–D). ABCA4, the photoreceptor ATP binding cassette transporter associated with retinoid transport (25), is primarily localized to rod and cone OSs (26). In AAV8(Y733F)-hGRK1-*mRd3*-treated 4Bnr *rd3* mice, ABCA4 immunolabeling is observed in both the outer and inner segments (Fig. 4E). As part of this study, we also investigated the distribution of cone arrestin in the retina of treated mice (Fig. 4F). Cone arrestin exhibited normal localization to cone OSs in light-adapted retinas.

Rescue of the rod but not cone photoresponse in AAV8(Y733F)-hGRK1-m*Rd3*-treated 4Bnr *rd3* mice as measured by ERGs

The effect of AAV8(Y733F)-hGRK1-*mRd3* treatment on the function of rod and cone photoreceptors of 4Bnr *rd3* mice was examined by light-elicited ERGs (Fig. 5A). At 1-week post-injection (P21), an attenuated dark-adapted scotopic ERG which

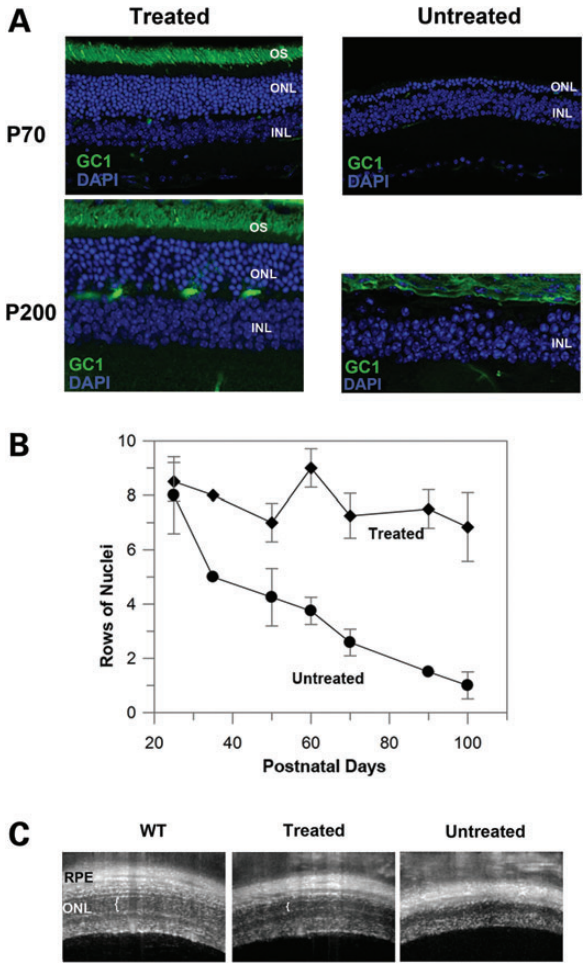

Figure 3. Prolonged GC1 expression and localization and sustained photoreceptor survival in AAV8(Y733F)-hGRK1-m*Rd3* treated mice. (**A**) Retinal sections of treated and untreated 4Bnr *rd3* mice injected at P14 were labeled for GC1 at P70 and P200. Normal localization of GC1 in the OS layer of treated mice was observed with a substantial ONL indicative of photoreceptor survival. No GC1 expression and significant loss (P70) or absence (P200) of the ONL layer was observed in the untreated retina. (**B**) Loss in the number of rows of photoreceptor nuclei in the ONL as a function of postnatal age for treated and untreated mice. Data are the mean ± SD for $n \geq 3$. (**C**) OCT image of WT, treated and untreated B4nr *rd3* mice injected at P14 and analyzed at P105. White vertical brackets designate the ONL observed in the retinas from WT and treated mice. No ONL was observed in the untreated mice. Representative micrographs are shown from analysis of four mice.

primarily measures the rod photoresponse was present in both the untreated and treated eyes with only minimal improvement in *a* and *b* wave amplitudes for the treated eye. At 3 months post-injection, the scotopic response was retained in the treated eye but no response was observed in the untreated eye. The *a* and *b* wave amplitudes of the treated and untreated eyes as a function of age are shown in Fig. 5B. The amplitude of the a wave was relatively stable following AAV8(Y733F)-hGRK1-*mrd3* treatment, while the amplitude of the *b* wave decreased to approximately half its value at early post-injection times before stabilizing. No photopic ERG response was observed for either the treated or untreated eye at any age (Fig. 5A).

To determine whether the absence of a photopic response in the 4Bnr *rd3* mice is due to the inability of AAV8(Y733F)-hGRK1-*mrd3*-treated *rd3* 4Bnr mice to stably express and translocate GC1 to cone OSs, we double-labeled retinal cryosections of WT, treated and untreated mice with cone opsin and GC1 antibodies (Fig. 6). The retinas of both the WT and 115-day post-injected mice showed strong GC1 expression of mid-wavelength cones in the OSs, indicating that long-term GC1 expression and trafficking to these cone OSs were normal. In contrast, essentially all the cone photoreceptors were lost in age-matched-untreated 4Bnr mice.

Immunofluorescence localization of GC1 in the 30Rk *rd3* mouse

It has been reported previously that the 4Bnr strain of *rd3* mice has an attenuated dark-adapted rod-derived response, but no light-adapted cone response at 24 days of age (10). In contrast, the In(5)30Rk/J strain (referred to here as 30Rk) has a small light-adapted photopic response, in addition to a dark-adapted scotopic response at 32 days of age. We reasoned that the 4Bnr *rd3* mice may have another defect that precludes the rescue of cone function by *Rd3* transgene expression.

Therefore, we have studied the 30Rk strain of *rd3* mice to determine (1) if GC1 expression and trafficking is defective in this strain of mice as observed for the 4Bnr strain, and (2) if gene delivery using AAV8(Y733F)-hGRK1-*mRd3* can rescue both rod and cone function and survival. We first examined the expression of GC1 in untreated 21-day-old 30Rk mice by immunofluorescence microscopy. Unlike the 4Bnr *rd3* strain, weak GC1 staining was detected in retinal cryosections of 30Rk mice labeled with an anti-GC1 polyclonal antibody (Fig. 7). Most GC1 labeling was observed within the photoreceptor inner segment layer where it co-localized with the anti-KDEL ER marker. Faint GC1 staining, however, was also seen in the OS layer, which may account for the attenuated ERG response observed in young 30Rk mice (10). For comparison, we stained retinal cryosections of WT mice for GC1 and KDEL-containing proteins. GC1 staining was restricted to the OS layer as expected, whereas intense KDEL staining of the ER was observed in the inner segment layer just above the ONL as well as in the RPE layer (Fig. 7).

Prolonged restoration of GC1 expression, photoreceptor survival and rod and cone function in the In(5)30Rk mice treated with AAV8(Y733F)-hGRK1-m*Rd3*

To determine whether the delivery of mouse *Rd3* gene can restore GC1 expression and rescue photoreceptors of the 30Rk mice, we injected AAV8(Y733F)-hGRK1-*mRd3* into the subretinal space of the right eyes of 14-day-old 30Rk mice and analyzed the expression 51 days later (P65). As in the case of the 4Bnr strain, strong endogenous GC1 expression was observed in the treated 30Rk strain laterally throughout the retina as visualized by immunofluorescence microscopy (Fig. 8A and B). At higher magnification, intense GC1 labeling was observed in the photoreceptor OSs of the treated eye, but only weak labeling was observed in the inner segments of the untreated eye (Fig. 8C and D). Prolonged expression and photoreceptor survival were also observed for this strain. At 7 months post-injection, the treated eyes showed strong GC1 immunofluorescence labeling in the OS layer and a prominent ONL having six to eight rows

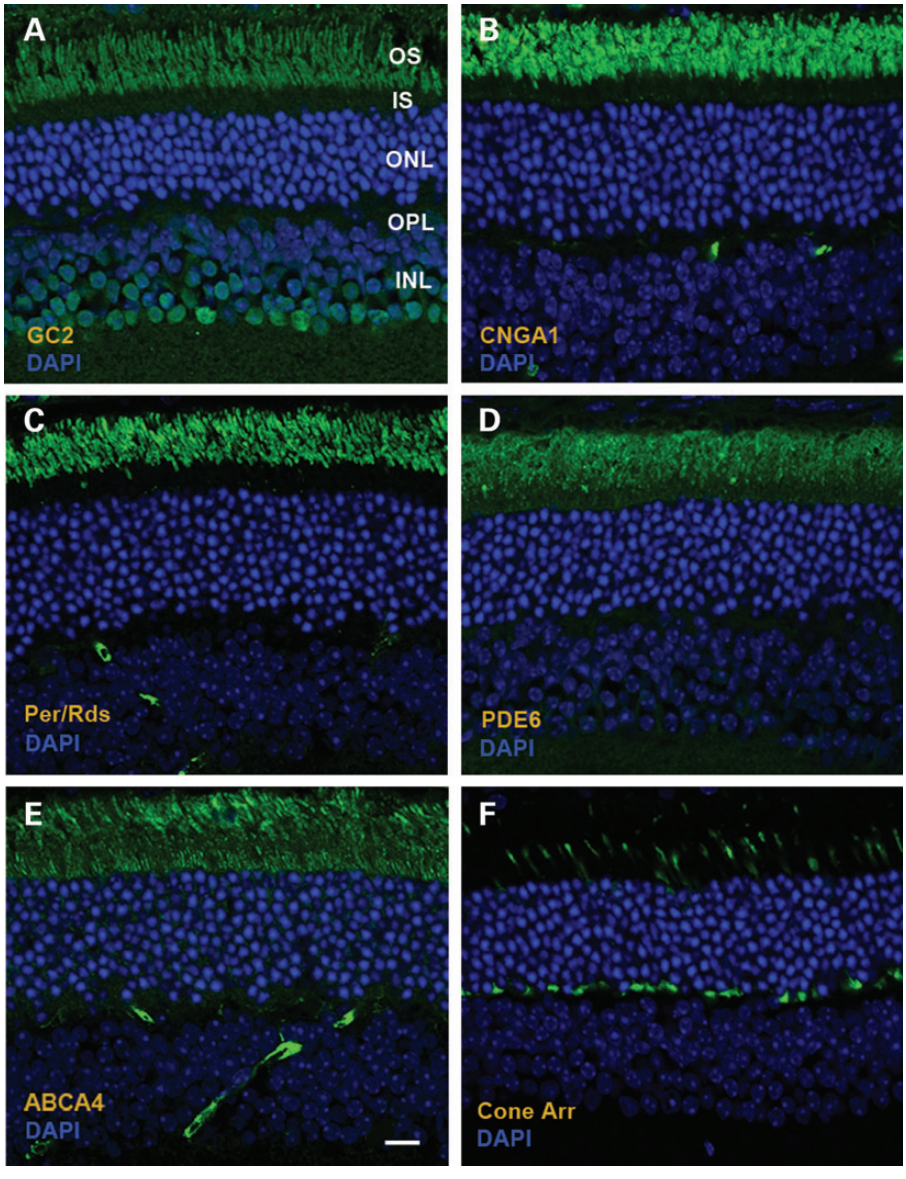

Figure 4. Distribution of photoreceptor proteins in AAV8(Y733F)-hGRK1-*mRd3*-treated 4Bnr *rd3* mice at 96 days post-injection (p110) as visualized by immunofluorescence microscopy. (**A**) GC2 labeling with an anti-GC2 polyclonal antibody; (**B**) Cyclic nucleotide-gated channel A1 subunit (CNGA1) labeling with the PMc 1D1 monoclonal antibody; (**C**) Peripherin/rds (Per/rds) labeling with the Per5H2 monoclonal antibody; (**D**) Rod phosphodiesterase alpha subunit (PDE6) labeling with an anti-PDE6A polyclonal antibody; (**E**) ABCA4 transporter labeling with the Rim 3F4 monoclonal antibody; (**F**) Cone arrestin labeling with a cone arrestin antibody. Representative micrographs are shown for two mice analyzed. Bar—10 μm.

of nuclei. In contrast, the untreated eye was reduced to a single layer (Fig. 8E and F).

To determine whether AAV-mediated *Rd3* delivery can preserve both rod and cone visual function, we measured the scotopic and photopic ERG response of the untreated and treated 30Rk mice. As illustrated in typical ERG recordings in Fig. 9A and B, there was a strong scotopic and phototopic response in the treated eye, and a significantly reduced scotopic and photopic response in the untreated eye at 51 days post-injection. In addition to the strong light-adapted photopic response, the treated eye showed a strong 12 Hz cone flicker response not observed in the untreated eye (Fig. 9C). The scotopic and photopic ERG response was also present in a cohort of mice at 5 months post-injection (Fig. 9D–F).

The photopic response observed in the treated 30Rk mice but absent in the treated 4Bnr mice could be due to a difference in the number of surviving cones. This was investigated by double labeling the retina of 30Rk mice at 6.5 months post-injection and 4Bnr mice at 4.5 months post-injection with anti-cone opsin and GC1 antibodies for analysis by confocal microscopy. Cone opsin was correctly localized to the OSs of all treated mice similar to that observed for WT mice (see Fig. 6). In contrast cone OSs were absent in the untreated mice and the few remaining cones showed sparse cone opsin labeling within the photoreceptor cell body, a pattern indicative of severe cone degeneration. The number of cones in the treated 30Rk and 4Bnr mice was compared (Fig. 9G). Similar numbers of cones were observed in the retina of the Rk30 and WT mice, whereas the number of

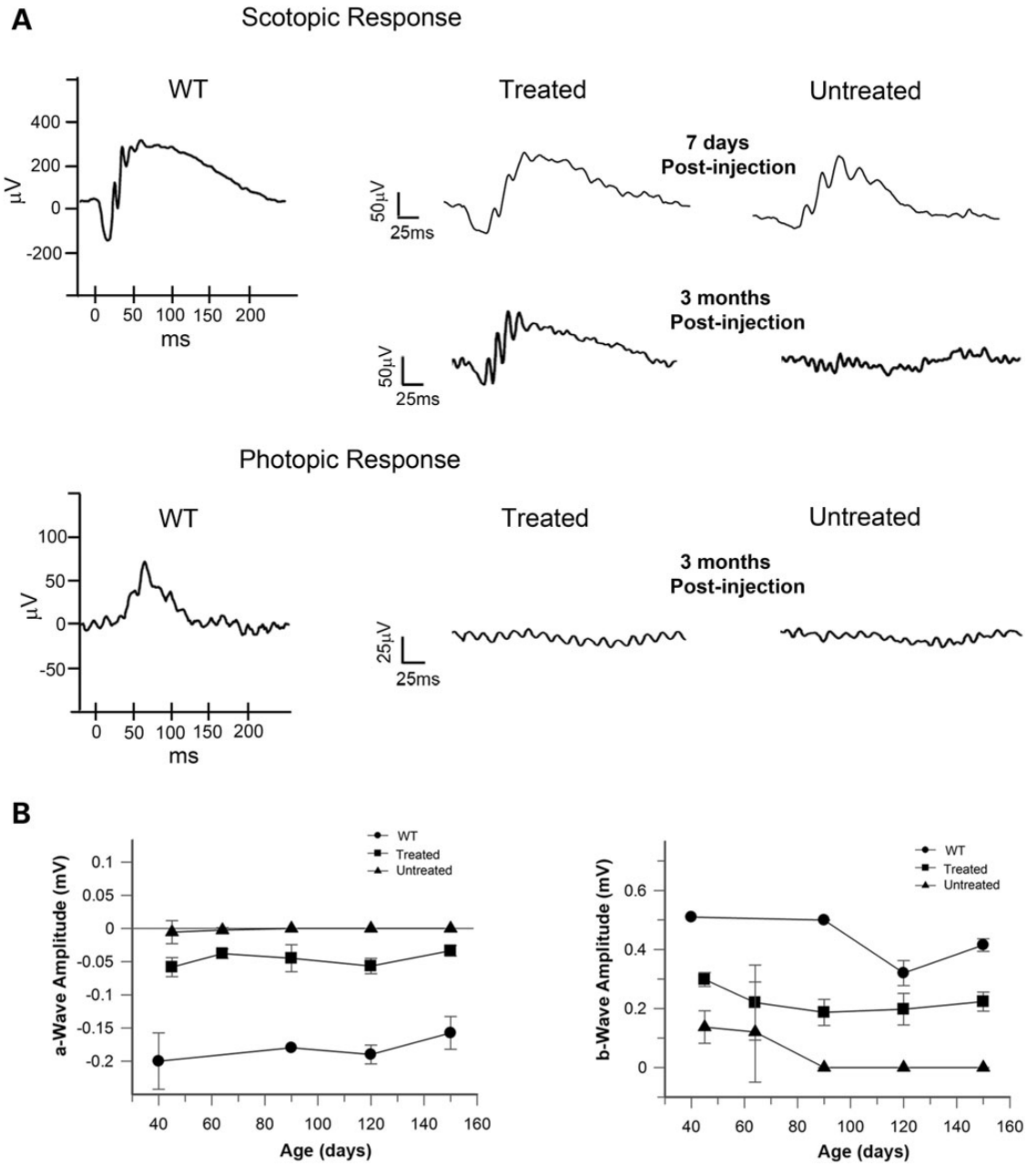

Figure 5. ERGs of AAV8(Y733F)-hGRK1-*mRd3*-treated and -untreated 4Bnr *rd3* mice. Mice were treated at P14 and their dark-adapted (scotopic) and light-adapted (photopic) ERGs were measured at various times after treatment. (**A**) Typical scotopic ERG ellicited at a light intensity of 2.25 cd s/m^2 and photopic ERG ellicited at a light intensity of 12 cd.s/m^2 in the presence of background light of 30 cd/m^2. Scotopic response was observed for the untreated and treated eyes at 7 days post-injection. At 3 months post-injection an ERG response was only observed for the treated eye. Photopic response was not observed at any age for the untreated or treated eyes. ERGs of WT are shown as a reference. (**B**) Effect of *a*-wave and *b*-wave amplitudes (mV) of the scotopic response as a function of the age of the WT, treated and untreated mice. Data are expressed as mean ± SD for $n \geq 3$.

cones in the 4Bnr mice was reduced by about 35%. The difference in the number of surviving cones between these strains is unlikely to account for the complete absence in photopic response in the treated 4Bnr mice.

DISCUSSION

In this study, we have employed self-complimentary AAV8(Y733F) to deliver the mouse *Rd3* cDNA to rod and cone photoreceptors of *rd3* mice in order to evaluate gene replacement therapy as a possible therapeutic treatment for LCA12 and gain further insight into the role of the RD3 protein in photoreceptor cells. A single subretinal injection of AAV8(Y733F)-hGRK1-*mRd3* into the eyes of 14 day old *rd3* mice resulted in rapid and strong expression of RD3 as measured by SDS gel electrophoresis and western blotting. We were unable to localize RD3 by immunofluorescence microscopy since the currently available anti-RD3 antibodies do not reliably

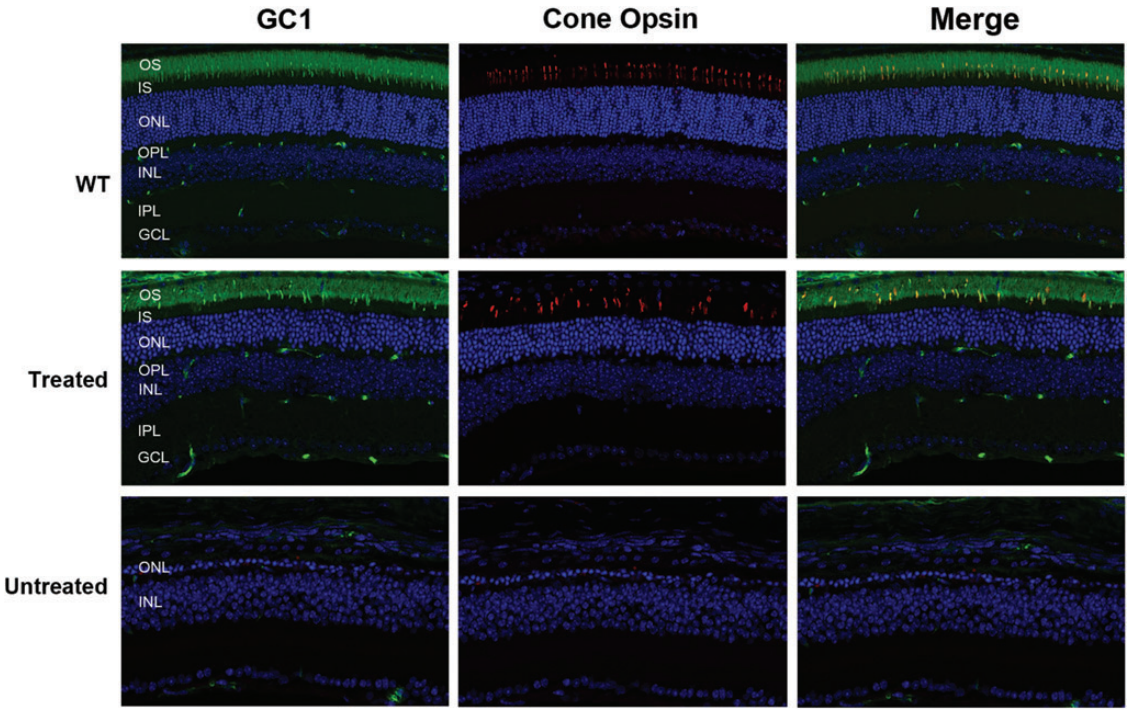

Figure 6. Presence of cone photoreceptors in the retina of AAV8(Y733F)-hGRK1-*mRd3*-treated and -untreated mice as visualized by immunofluorescence microscopy. Retinal cryosections from WT mice and the treated and untreated 4Bnr mice were were double labeled for GC1 and middle wavelength cone opsin. Both the WT and treated mice showed a significant number of cone photoreceptor cells with cone opsin and GC1 co-localized to the OSs (merged image). The treated mice were injected at P14 and analyzed 115 days later. No significant labeling was observed for the untreated 4Bnr mice indicative of extensive cone degeneration. Representative micrographs are shown from the analysis of six 4Bnr mice and three WT mice analyzed.

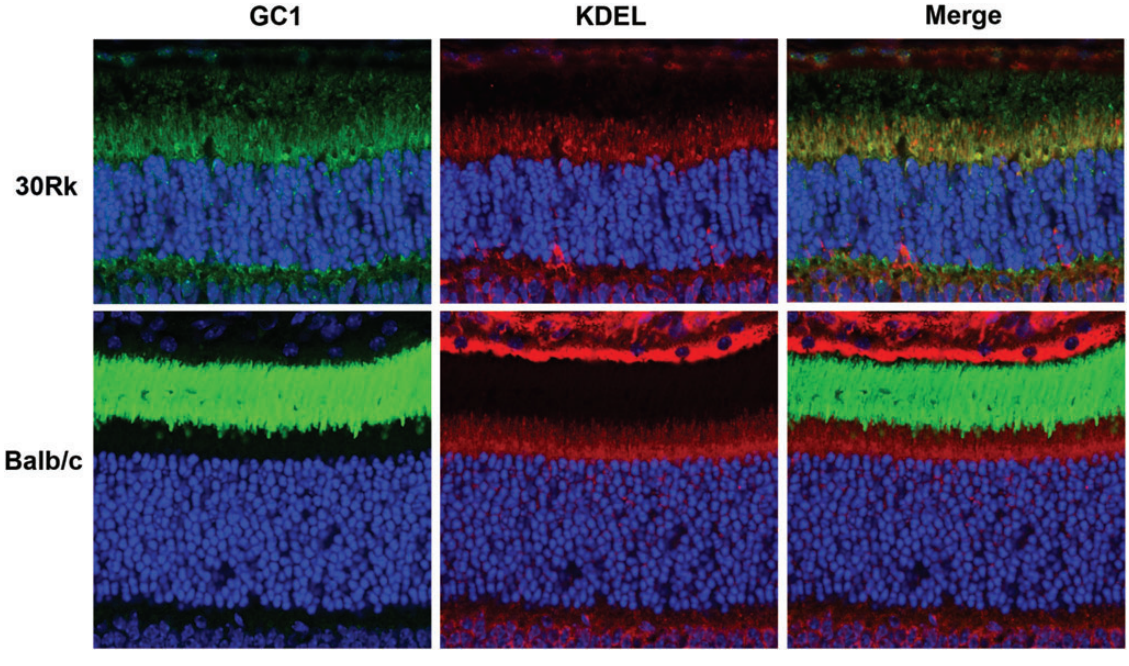

Figure 7. Localization of GC1 in the retina of untreated 21-day-old 30Rk mouse. GC1 labeling is predominantly found in the inner segment where it co-localizes with the anti-KDEL ER marker. Weak GC1 labeling is also detected in the OSs and outer plexiform layers. Labeling of a retina from WT (Balb/c) mice is shown for comparison with intense GC1 labeling detectable only in the OS and KDEL labeling in the inner segment. Representative micrographs are shown from the analysis of two WT and two 30Rk mice.

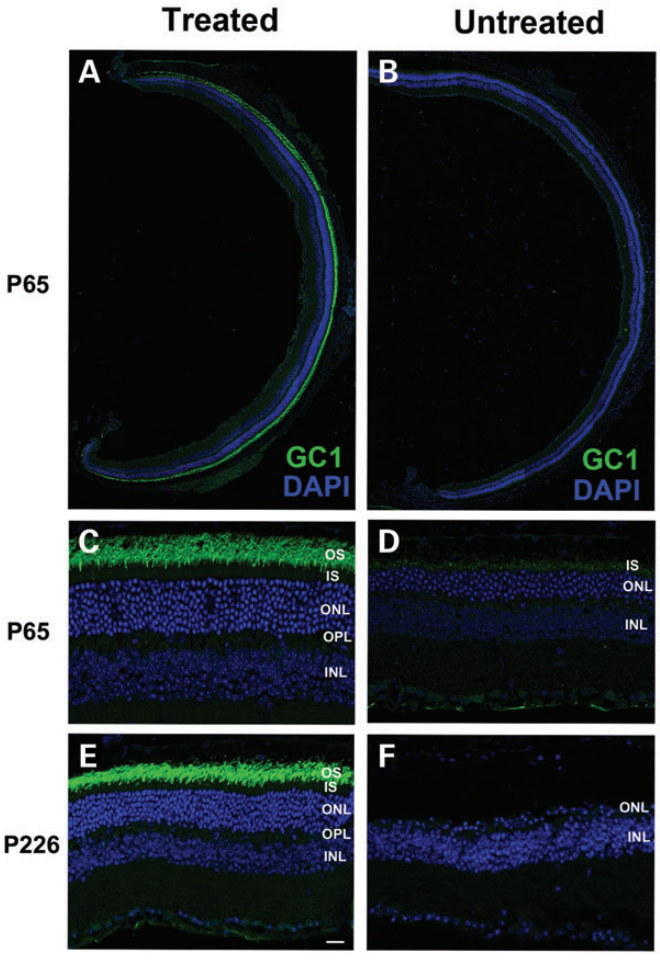

Figure 8. GC1 expression and localization in the photoreceptors of AAV8(Y733F)-hGRK1-*mRd3*-treated and -untreated 30Rk-*rd3* mice. The treated right eye was injected at P14 with the untreated left eye serving as a contralateral control. Retinal cryosections were prepared at P65 and labeled with a polyclonal antibody to GC1 and counterstained with DAPI. (**A** and **B**) Retinal sections of a treated and untreated eye labeled for GC1. Intense endogenous GC1 immunostaining is present laterally throughout the retina of the treated eye (A) and only faint immunostaining observed in the untreated eye (B). (**C** and **D**) At higher magnification, GC1 labeling is restricted to the OS layer of the treated eye (**C**). Faint labeling of GC1 in the untreated eye is observed primarily in the inner segment (**D**). (**E** and **F**) Labeling of a treated and untreated eye at P226, ~7 months post-injection. The retina of the treated eye showed intense GC1 labeling in the OS layer and a substantial DAPI stained ONL (**E**). In contrast, the untreated eye showed a single row of nuclei in the ONL (**F**). Representative micrographs are shown from the analysis of six mice. Bar—20 μm.

label retinal cryosections above the background. Nonetheless, transgene expression of RD3 led to the strong expression and efficient translocation of endogenous GC1 and GC2 to rod and cone OSs across most of the retina as visualized by confocal scanning microscopy. This provides strong evidence for a crucial role of RD3 in GC expression and localization in photoreceptors. Importantly, RD3-induced GC expression and trafficking to OSs coincided with prolonged restoration of visual function as measured by ERGs and photoreceptor survival as observed by the thickness of the ONL.

The self-complimentary AAV8 with a Y733F capsid mutation efficiently transduces mouse photoreceptors and leads to rapid, high protein expression within 1 week after injection. This is a substantial improvement over AAV5 which has a strong tropism for mouse photoreceptors, but displays a relatively long latent period of 4–6 weeks before significant protein expression is observed (27, 28). The human rhodopsin kinase (hGRK1) promoter in conjunction with AAV8(Y733F) has been successfully used to restore rod and cone function in GC knockout mice and *Aipl1* null mice (18, 20). The hGRK1 promoter has also been reported to induce protein expression in rod and cone photoreceptors of nonhuman primates (29).

Previous studies have shown that the 4Bnr and 30Rk strains of *rd3* mice both harboring a stop mutation at codon 107 of the endogenous *Rd3* gene differ in their rate of photoreceptor degeneration and ERG response prior to significant photoreceptor cell loss (10, 22). The 30Rk strain has a slower rate of photoreceptor cell death and exhibits an attenuated scotopic and photopic ERG response within the first month of life. In contrast, photoreceptors of the 4Bnr strain degenerate more quickly and display a diminished scotopic response but no photopic response within the first month of life. Subretinal delivery of AAV8(Y733F)-hGRK1-*mRd3* led to strong expression of GC in rods and cones and enhanced photoreceptor cell survival in both strains of mice. However, only the 30Rk strain showed strong recovery of the light-adapted photopic ERG and 12 Hz flicker characteristic of cone-derived photoresponse. The failure of the 4Bnr strain to generate a cone-mediated ERG after *Rd3* gene delivery suggests that these mice may have another defect which adversely affects phototransduction in cone cells. The 4Bnr strain is known to have a Robertsonian translocation (30). This chromosomal aberration or a loss in function mutation in a gene encoding another key protein associated with the cone photoresponse may be responsible for the inability of *Rd3* gene delivery to rescue cone function in the 4Bnr *rd3* mice.

To date all *RD3* mutations associated with severe photoreceptor degeneration in animals and humans are predicted to encode an unstable C-terminal truncated protein. The mutation in the *rd3* mouse produces a 106 amino acid truncated protein which is highly unstable and unable to interact with GC (10, 14, 15). The genetic defect in the *rcd2* collie involves an insertion which alters the last 61 codons of the normal gene (13). Affected canines display early-onset night blindness, abnormal rod and cone OSs, and initial loss in rod photoreceptors followed by degeneration of cones with functional blindness at 6–8 months of age (31). Interestingly, early biochemical studies indicate that affected dogs exhibit a 10-fold increase in cGMP between postnatal day 20–40, suggesting that GC is expressed and active at early ages in this model (31). It remains to be determined how the mutated RD3 protein affects GC expression and localization in this canine model. Truncation mutations in *RD3* have been found in a number of LCA12 families. An Indian family was first identified with an alteration in an invariant G nucleotide at the end of exon 2 donor splice site of *RD3* resulting in a stop codon following codon 99 (10). A Kurdish family was subsequently reported to display a premature stop codon at Position 60 (11). Most recently, an international effort has identified three new RD3 truncation mutations in unrelated LCA12 families (12). Clinical analyses indicate that affected members of these families experience early and severe vision loss associated with degeneration of both rod and cone photoreceptors and phenotypic features commonly found in LCA1 patients with mutations in GC1.

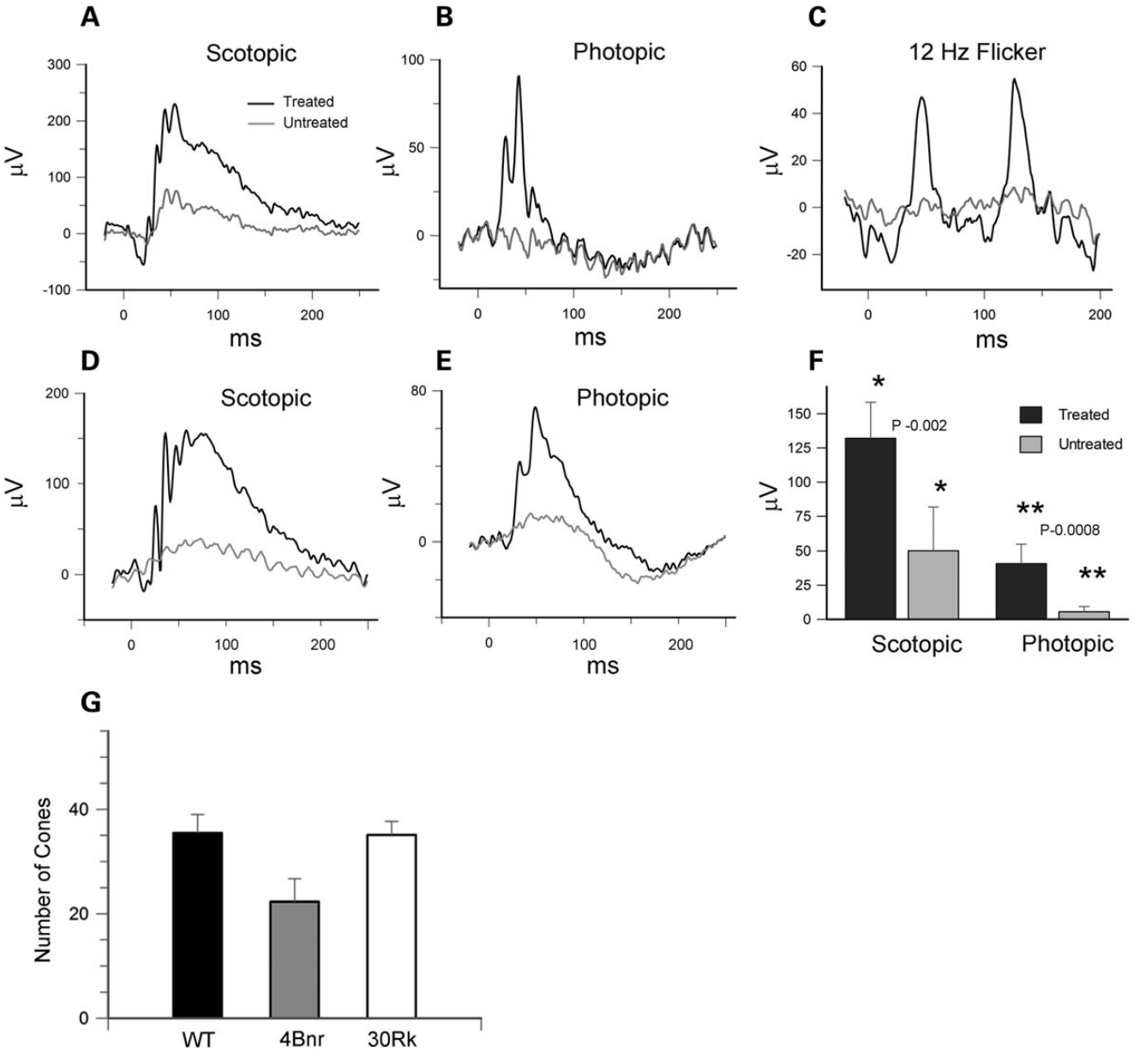

Figure 9. ERGs of 30Rk-*rd3* mice treated with AAV8(Y733F)-hGRK1-*mRd3* at P14 and analyzed at P65 and P150. (**A**) Scotopic ERG response of the AAV treated and untreated eyes ellicited at a light intensity of 2.25 cd s/m^2 for a 30Rk mouse at P65. (**B**) Photopic ERG response ellicited at a light intensity of 12 cd s/m^2 in the presence of background light of 30 cd/m^2 at P65. (**C**) The 12 Hz flicker response for the treated and untreated eyes at P65. (**D** and **E**) An example of the scotopic and photopic response for the treated and untreated eye for a 30Rk mouse at P150. (**F**) Differences in scotopic and photopic *b*-wave amplitudes for mice at 5-month post-injection. Data are expressed as mean $\pm$ SD for $n = 6$. Mean values within each group for the ERG response was compared using a standard paired Student's *t*-test. (**G**) The number of cones was determined for WT and AAV-treated 30Rk mice 6.5 months postinjection and 4Bnr mice 4.5 months postinjection over 300 μm length of retina. Data are expressed as mean $\pm$ SD for $n = 5$. A multigroup statistical test described in the Materials and Methods section was used to compare groups ($P = 0.009$).

Analysis of the 4Bnr and 30Rk strains of *rd3* mice provide new insight into the mechanism by which RD3 promotes stable GC expression and localization in photoreceptors. Although GC expression is undetectable in the untreated 4Bnr strain as previously shown (14) and confirmed in this study, low GC1 immunolabeling is observed in photoreceptor inner segments and, to a lesser extent, OSs of 21-day old untreated 30Rk *rd3* mice by confocal scanning microscopy. GC1 labeling in the inner segment co-localizes with the anti-KDEL antibody which serves as a reliable ER marker. This indicates that in the absence of functional RD3, most of the GC1 fails to efficiently exit the ER and is degraded reflecting the faint GC labeling. A residual amount of GC exits the ER and translocates to the OS. This low level of GC may account for the attenuated rod and cone ERG response which is observed in the young 30Rk *rd3* mice but not observed in GC1/GC2 double knockout mice (4). AAV-mediated delivery and expression of RD3 facilitates the exit of GC1 from the ER and its translocation to rod and cone photoreceptor OSs. These findings are in general agreement with heterologous over expression studies which showed that GC1 is retained in the ER of COS-7 cells in

the absence of RD3, but exits the ER when co-expressed with RD3 (14).

RD3 has been shown to inhibit GC catalytic activity (15). The earlier findings that *rcd2* pups exhibit high cGMP levels may be explained on the basis of the loss in RD3-mediated GC inhibition together with limited GC expression. The high cGMP levels generated by mislocalized GC in the inner segment could cause photoreceptor cell death. However, analysis of the two strains of *rd3* mice suggests that this is not a major contribution to photoreceptor degeneration. More specifically, the 30Rk mice which display a detectable level of GC in the inner segments degenerate more slowly than the 4Bnr mice showing no detectable GC by SDS gels or immunofluorescence microscopy. More likely, photoreceptor degeneration is caused by the absence of GC in the OSs and its impact on calcium homeostasis (14, 32), although other mechanisms may also contribute to photoreceptor degeneration.

The rescue of photoreceptor OS GC expression and ERG response indicates that phototransduction is operational in the AAV8(Y733F)-hGRK1-*mRd3*-treated *rd3* mice. Analysis of cortical and subcortical visual functions as analyzed by the Morris water maze and virtual optokinetic test was beyond the scope of the present study. Recently, however, cortical and subcortical visual behavior together with ERGs has been rescued by AAV-mediated delivery of mouse GC1 to photoreceptor cells of GC1/GC2 double knockout mice (33). Since the GC1/GC2 double knockout mouse is phenotypically similar to the *rd3* mouse, it is likely that the cortical and subcortical visual behavior is preserved in AAV-treated *rd3* mice in this study, although this needs to be verified in future studies.

In summary, our results provide strong evidence for the function of RD3 as a chaperone trafficking protein, which facilitates the exit of GC from the ER. In the absence of RD3, GC is primarily retained in the ER and rapidly degraded. The absence of GC in photoreceptor OSs results in the loss in visual function and photoreceptor degeneration observed in the *rd3* mouse and most likely the *rcd2* collie and LCA12 patients. AAV-mediated gene delivery to the *rd3* mouse leads to enhanced expression and localization of GC to photoreceptor OSs via RD3 chaperone activity and the recovery of visual function and sustained photoreceptor survival.

MATERIALS AND METHODS

Experimental animals

Rd3 strain Rb(11.13)4Bnr/J (4Bnr) and In(5)30Rk/J (30Rk) and control Balb/c mice were obtained from Jackson Laboratory (Bar Harbor, ME) and bred and maintained at the University of British Columbia under a 12 h light/dark cycle. All experiments were conducted in accordance with the ARVO Statement for the Use of Animals in Ophthalmic and Vision Research and protocols were approved by the UBC Committee on Animal Care.

AAV vectors and subretinal injections

AAV8 vector containing the surface exposed Y733F mutation in the capsid protein and containing the murine *Rd3* cDNA under the control of the photoreceptor-specific human G-protein-coupled kinase 1 (GRK1) promoter was prepared as previously described (17, 34, 35). The titer of the AAV8(Y733F)-GRK1-*Rd3* was 1.0×10^{13} vector genomes/ml.

One microliter of vector containing between 1×10^9 to 5×10^9 vector genomes was injected subretinally into the right eyes of post-natal day 14 (P14) *rd3* mice placed under general anesthesia as previously described (27). The left eye was not injected and served as a contralateral control.

Optical coherence topography (OCT) and electroretinographic (ERG) analysis

OCT was carried out as previously described (36). Measurements were typically made between P28-P40 and used to eliminate any retinas that were detached or had any other complications caused by the injection. Scotopic and photopic ERGs were performed on mice under anesthesia as previously described (27) and analyzed on an Espion System; Diagnosys (621 Software version). Briefly, the pupils of dark-adapted mice anesthetized by subcutaneous injections of ketamine (72 mg/kg)/xylazine (5 mg/kg) were dilated with 1% isopto atropine under dim red light. Dark-adapted ERGs were initiated with light flashes of various light intensities with most studies being carried out at 2.25 cd.s/m^2. Light-adapted cone responses were elicited in the presence of 30 cd/m^2 background light. Variable light flash intensities were used with most studies being carried out at 12 cd.s/m^2. ERG data were presented as mean $\pm$ standard deviation. Statistical significance for comparison of amplitudes was determined using a paired statistical *t*-test. Significance was defined as a *P*-value of <0.05.

Antibodies and immunocytochemistry

The following antibodies to photoreceptor proteins were used: monoclonal antibody PMc-1D1 against the rod cyclic nucleotide-gated channel A1 subunit (CNGA1) (37) as a stock cell culture supernatant (dilution 1 : 10); monoclonal antibody Rd3-9D12 against RD3 as a stock cell culture supernatant (dilution 1 : 5); polyclonal antibody pAb-63 against RD3 as a purified stock solution at 0.2 mg Ab/ml (dilution 1 : 2000) (14); polyclonal antibody to guanylate cyclases GC1 and GC2 (generous gift from the late David Garbers) as stock serum (dilution 1 : 2000); monoclonal antibody GC-8A5 to GC1 generated as part of this project as a stock cell culture supernatant (dilution 1 : 3); polyclonal antibody to guanylate cyclase activating protein-1 (GCAP1) (a generous gift from Wolfgang Baehr of the University of Utah) (dilution 1 : 20,000); polyclonal antibody to PDE6(α) from Affinity BioReagents (dilution 1 : 500); polyclonal antibodies to M/L opsin from Millipore (Temecula, CA) (dilution 1 : 2000); polyclonal antibody to β-actin (Abcam) (dilution 1 : 1000); antibody to cone arrestin (Millipore) (dilution 1 : 2000) and monoclonal antibody to KDEL (Stressgen) (dilution 1 : 100).

Immunofluorescence microscopy was carried out on retinal cryosections as previously described (9, 38). Briefly, injected and uninjected eyes from 4Bnr and 30Rk *rd3* were fixed for 2 h in 4% paraformaldehyde, 0.1 M phosphate buffer pH 7.3. Cryosections (10–12 μm) were permeabilized and blocked with 0.2% Triton X-100 and 10% normal goat serum and labeled overnight with a primary antibody and subsequently labeled with a secondary antibody conjugated with Alexa 488 or 594. Sections were counterstained with 4′,6-diamidino-2-phenylindole (DAPI)

nuclear stain and visualized on a Zeiss LSM700 confocal microscope. Images were analyzed using Zeiss Zen software.

Analysis of cone photoreceptors

The number and viability of cone photoreceptors were determined in AAV-treated 4Bnr and 30RK mice on retinal cryosections double labeled for GC1 and cone opsin and compared with the number of cones in WT mice. The mean number of cones per unit length across the retina was determined by averaging the number of labeled cones over a distance of 300 μm in the nasal, central and temporal regions of the retina. Data were shown as a mean ± SD for $n = 5$. A non-parametric Kruskal–Wallis statistical test followed by *post hoc* test was applied for multigroup statistical analysis. Cone opsin labeling was observed in the OSs of WT and treated mice showing GC1 expression, but was delocalized to the cell bodies of the few residual cones present in the untreated mice.

Retinal extracts and western blotting

Three 35 day post-injected 4Bnr mice and three age-matched control Balb/c mice were sacrificed and their eyes were enucleated. Six retinas from each cohort were removed from the eyecup and immersed in 400 μl Tris buffer saline (TBS: 20 mm Tris, pH 7.4, 0.1 M NaCl and cOmplete protease inhibitor (Roche)) for 20 min on ice. A retinal cell extract was prepared by passing the suspension through a 22 g and 28 g needle. The extract (400 μl) was layered on top of 1.6 ml of 60% (w/w) sucrose/TBS and centrifuged at 25 000 rpm for 30 min in a TLS-55 rotor in a Beckman TLX Optima centrifuge. The retinal membrane fraction which banded on top of the 60% sucrose was removed, diluted with 3 volumes of TBS, and pelleted by centrifugation at 30 000 rpm for 10 min in a TLA 100.4 rotor. The membranes were resuspended with 100 μl of TBS. The protein concentration was determined by BCA assay (Pierce) and an aliquot of 20 μg of the membrane extract from the injected mice and control mice sample solubilized in SDS containing 2-mercaptoethanol was run on a NuPage 4–12% gradient gel, and transferred onto PVDF Immobilon-FL(Millipore) membrane. The blots were blocked in 1% milk/PBS and subsequently labeled for 1 h with primary antibodies MAb GC1-8A5 and RD3-9D12, and PAb anti-β actin as a loading control. Either goat anti-mouse or goat anti-rabbit conjugated to IRdye 680 was applied for 1 h, and after three washings with PBS-Tween20, blots were imaged on an Odyssey Licor infrared imaging system.

ACKNOWLEDGEMENTS

The authors thank Andrew Metcalfe for technical assistance with the initial ERG recordings and Santhi Mani with AAV vector plasmid construction. This work was supported by grants from the Canadian Institutes for Health Research/Foundation Fighting Blindness—Canada (grant no. CIHR RMF-92101), the National Institutes of Health [grant no. EY002422; EY021721], the Macula Vision Research Foundation, and Research to Prevent Blindness. R.S.M. holds a Canada Research Chair in Vision and Macular Degeneration.

Conflict of Interest statement. W.W.H. and the University of Florida have a financial interest in the use of AAV therapies, and own equity in a company (AGTC Inc.) that might, in the future, commercialize some aspects of this work.

REFERENCES

1. den Hollander, A.I., Roepman, R., Koenekoop, R.K. and Cremers, F.P. (2008) Leber congenital amaurosis: genes, proteins and disease mechanisms. *Prog. Retin. Eye Res.*, **27**, 391–419.
2. Perrault, I., Rozet, J.M., Calvas, P., Gerber, S., Camuzat, A., Dollfus, H., Chatelin, S., Souied, E., Ghazi, I., Leowski, C. *et al.* (1996) Retinal-specific guanylate cyclase gene mutations in Leber's congenital amaurosis. *Nat. Genet.*, **14**, 461–464.
3. Yang, R.B. and Garbers, D.L. (1997) Two eye guanylyl cyclases are expressed in the same photoreceptor cells and form homomers in preference to heteromers. *J. Biol. Chem.*, **272**, 13738–13742.
4. Baehr, W., Karan, S., Maeda, T., Luo, D.G., Li, S., Bronson, J.D., Watt, C.B., Yau, K.W., Frederick, J.M. and Palczewski, K. (2007) The function of guanylate cyclase 1 and guanylate cyclase 2 in rod and cone photoreceptors. *J. Biol. Chem.*, **282**, 8837–8847.
5. Shyjan, A.W., de Sauvage, F.J., Gillett, N.A., Goeddel, D.V. and Lowe, D.G. (1992) Molecular cloning of a retina-specific membrane guanylyl cyclase. *Neuron*, **9**, 727–737.
6. Luo, D.G., Xue, T. and Yau, K.W. (2008) How vision begins: an odyssey. *Proc. Natl Acad. Sci. USA*, **105**, 9855–9862.
7. Burns, M.E. and Arshavsky, V.Y. (2005) Beyond counting photons: trials and trends in vertebrate visual transduction. *Neuron*, **48**, 387–401.
8. Lowe, D.G., Dizhoor, A.M., Liu, K., Gu, Q., Spencer, M., Laura, R., Lu, L. and Hurley, J.B. (1995) Cloning and expression of a second photoreceptor-specific membrane retina guanylyl cyclase (RetGC), RetGC-2. *Proc. Natl Acad. Sci. USA*, **92**, 5535–5539.
9. Kwok, M.C., Holopainen, J.M., Molday, L.L., Foster, L.J. and Molday, R.S. (2008) Proteomics of photoreceptor outer segments identifies a subset of SNARE and Rab proteins implicated in membrane vesicle trafficking and fusion. *Mol. Cell Proteomics*, **7**, 1053–1066.
10. Friedman, J.S., Chang, B., Kannabiran, C., Chakarova, C., Singh, H.P., Jalali, S., Hawes, N.L., Branham, K., Othman, M., Filippova, E. *et al.* (2006) Premature truncation of a novel protein, RD3, exhibiting subnuclear localization is associated with retinal degeneration. *Am. J. Hum. Genet.*, **79**, 1059–1070.
11. Preising, M.N., Hausotter-Will, N., Solbach, M.C., Friedburg, C., Ruschendorf, F. and Lorenz, B. (2012) Mutations in RD3 are associated with an extremely rare and severe form of early onset retinal dystrophy. *Invest. Ophthalmol. Vis. Sci.*, **53**, 3463–3472.
12. Perrault, I., Estrada-Cuzcano, A., Lopez, I., Kohl, S., Li, S., Testa, F., Zekveld-Vroon, R., Wang, X., Pomares, E., Andorf, J. *et al.* (2013) Union makes strength: a worldwide collaborative genetic and clinical study to provide a comprehensive survey of RD3 mutations and delineate the associated phenotype. *PLoS One*, **8**, e51622.
13. Kukekova, A.V., Goldstein, O., Johnson, J.L., Richardson, M.A., Pearce-Kelling, S.E., Swaroop, A., Friedman, J.S., Aguirre, G.D. and Acland, G.M. (2009) Canine RD3 mutation establishes rod-cone dysplasia type 2 (rcd2) as ortholog of human and murine rd3. *Mamm. Genome*, **20**, 109–123.
14. Azadi, S., Molday, L.L. and Molday, R.S. (2010) RD3, the protein associated with Leber congenital amaurosis type 12, is required for guanylate cyclase trafficking in photoreceptor cells. *Proc. Natl Acad. Sci. USA*, **107**, 21158–21163.
15. Peshenko, I.V., Olshevskaya, E.V., Azadi, S., Molday, L.L., Molday, R.S. and Dizhoor, A.M. (2011) Retinal degeneration 3 (RD3) protein inhibits catalytic activity of retinal membrane guanylyl cyclase (RetGC) and its stimulation by activating proteins. *Biochemistry*, **50**, 9511–9519.
16. Karan, S., Frederick, J.M. and Baehr, W. (2010) Novel functions of photoreceptor guanylate cyclases revealed by targeted deletion. *Mol. Cell. Biochem.*, **334**, 141–155.
17. Petrs-Silva, H., Dinculescu, A., Li, Q., Min, S.H., Chiodo, V., Pang, J.J., Zhong, L., Zolotukhin, S., Srivastava, A., Lewin, A.S. *et al.* (2009) High-efficiency transduction of the mouse retina by tyrosine-mutant AAV serotype vectors. *Mol. Ther.*, **17**, 463–471.

18. Ku, C.A., Chiodo, V.A., Boye, S.L., Goldberg, A.F., Li, T., Hauswirth, W.W. and Ramamurthy, V. (2011) Gene therapy using self-complementary Y733F capsid mutant AAV2/8 restores vision in a model of early onset Leber congenital amaurosis. *Hum. Mol. Genet.*, **20**, 4569–4581.
19. Pang, J.J., Dai, X., Boye, S.E., Barone, I., Boye, S.L., Mao, S., Everhart, D., Dinculescu, A., Liu, L., Umino, Y. *et al.* (2011) Long-term retinal function and structure rescue using capsid mutant AAV8 vector in the rd10 mouse, a model of recessive retinitis pigmentosa. *Mol. Ther.*, **19**, 234–242.
20. Boye, S.L., Conlon, T., Erger, K., Ryals, R., Neeley, A., Cossette, T., Pang, J., Dyka, F.M., Hauswirth, W.W. and Boye, S.E. (2011) Long-term preservation of cone photoreceptors and restoration of cone function by gene therapy in the guanylate cyclase-1 knockout (GC1KO) mouse. *Invest. Ophthalmol. Vis. Sci.*, **52**, 7098–7108.
21. Chang, B., Heckenlively, J.R., Hawes, N.L. and Roderick, T.H. (1993) New mouse primary retinal degeneration (rd-3). *Genomics*, **16**, 45–49.
22. Linberg, K.A., Fariss, R.N., Heckenlively, J.R., Farber, D.B. and Fisher, S.K. (2005) Morphological characterization of the retinal degeneration in three strains of mice carrying the rd-3 mutation. *Vis. Neurosci.*, **22**, 721–734.
23. Dizhoor, A.M., Olshevskaya, E.V. and Peshenko, I.V. (2010) Mg2+/Ca2+ cation binding cycle of guanylyl cyclase activating proteins (GCAPs): role in regulation of photoreceptor guanylyl cyclase. *Mol. Cell. Biochem.*, **334**, 117–124.
24. Gorczyca, W.A., Gray-Keller, M.P., Detwiler, P.B. and Palczewski, K. (1994) Purification and physiological evaluation of a guanylate cyclase activating protein from retinal rods. *Proc. Natl Acad. Sci. USA*, **91**, 4014–4018.
25. Quazi, F., Lenevich, S. and Molday, R.S. (2012) ABCA4 Is an *N*-retinylidene-phosphatidylethanolamine and phosphatidylethanolamine importer. *Nat. Commun.*, **3**, 925.
26. Molday, L.L., Rabin, A.R. and Molday, R.S. (2000) ABCR Expression in foveal cone photoreceptors and its role in Stargardt macular dystrophy. *Nat. Genet.*, **25**, 257–258.
27. Min, S.H., Molday, L.L., Seeliger, M.W., Dinculescu, A., Timmers, A.M., Janssen, A., Tonagel, F., Tanimoto, N., Weber, B.H., Molday, R.S. *et al.* (2005) Prolonged recovery of retinal structure/function after gene therapy in an Rs1h-deficient mouse model of x-linked juvenile retinoschisis. *Mol. Ther.*, **12**, 644–651.
28. Janssen, A., Min, S.H., Molday, L.L., Tanimoto, N., Seeliger, M.W., Hauswirth, W.W., Molday, R.S. and Weber, B.H. (2008) Effect of late-stage therapy on disease progression in AAV-mediated rescue of photoreceptor cells in the retinoschisin-deficient mouse. *Mol. Ther.*, **16**, 1010–1017.
29. Boye, S.E., Alexander, J.J., Boye, S.L., Witherspoon, C.D., Sandefer, K.J., Conlon, T.J., Erger, K., Sun, J., Ryals, R., Chiodo, V.A. *et al.* (2012) The human rhodopsin kinase promoter in an AAV5 vector confers rod- and cone-specific expression in the primate retina. *Hum. Gene Ther.*, **23**, 1101–1115.
30. Everett, C.A., Searle, J.B. and Wallace, B.M. (1996) A study of meiotic pairing, nondisjunction and germ cell death in laboratory mice carrying robertsonian translocations. *Genet Res*, **67**, 239–247.
31. Woodford, B.J., Liu, Y., Fletcher, R.T., Chader, G.J., Farber, D.B., Santos-Anderson, R. and Tso, M.O. (1982) Cyclic nucleotide metabolism in inherited retinopathy in collies: a biochemical and histochemical study. *Exp. Eye Res.*, **34**, 703–714.
32. Fain, G.L. (2006) Why photoreceptors die (and why they don't). *Bioessays*, **28**, 344–354.
33. Boye, S.L., Peshenko, I.V., Huang, W.C., Min, S.H., McDoom, I., Kay, C.N., Liu, X., Dyka, F.M., Foster, T.C., Umino, Y. *et al.* (2013) AAV-mediated gene therapy in the guanylate cyclase (RetGC1/RetGC2) double knockout mouse model of Leber congenital amaurosis. *Hum. Gene Ther.*, **24**, 189–202.
34. Zhong, L., Li, B., Mah, C.S., Govindasamy, L., Agbandje-McKenna, M., Cooper, M., Herzog, R.W., Zolotukhin, I., Warrington, K.H. Jr., Weigel-Van Aken, K.A. *et al.* (2008) Next generation of adeno-associated virus 2 vectors: point mutations in tyrosines lead to high-efficiency transduction at lower doses. *Proc. Natl Acad. Sci. USA*, **105**, 7827–7832.
35. Zolotukhin, S., Potter, M., Zolotukhin, I., Sakai, Y., Loiler, S., Fraites, T.J. Jr., Chiodo, V.A., Phillipsberg, T., Muzyczka, N., Hauswirth, W.W. *et al.* (2002) Production and purification of serotype 1, 2, and 5 recombinant adeno-associated viral vectors. *Methods*, **28**, 158–167.
36. Xu, J., Molday, L.L., Molday, R.S. and Sarunic, M.V. (2009) In vivo imaging of the mouse model of X-linked juvenile retinoschisis with fourier domain optical coherence tomography. *Invest. Ophthalmol. Vis. Sci.*, **50**, 2989–2993.
37. Cook, N.J., Molday, L.L., Reid, D., Kaupp, U.B. and Molday, R.S. (1989) The cGMP-gated channel of bovine rod photoreceptors is localized exclusively in the plasma membrane. *J. Biol. Chem.*, **264**, 6996–6999.
38. Cheng, C.L., Djajadi, H. and Molday, R.S. (2013) Cell-specific markers for the identification of retinal cells by immunofluorescence microscopy. *Methods Mol. Biol.*, **935**, 185–199.